AARHUS UNIVERSITY

quanTEEM
ERASMUS MUNDUS MASTER
QUANTUM TECHNOLOGIES
AND ENGINEERING

Magnetization in Antiferromagnetic Heisenberg Lattices

Individual Physics Project (5 ECTS)

Supervisor: Prof. Dr. Georg Bruun

January 23, 2026

B. E. Castiblanco[1]

MSc Physics – Erasmus Mundus Master in Quantum Technologies and Engineering
QuanTEEM

Center for Complex Quantum Systems
Department of Physics and Astronomy
Aarhus University

[1] au786622@uni.au.dk

Abstract

It is shown a theoretical and computational study of the antiferromagnetic order in frustrated spin-1/2 Heisenberg models in the nearest-neighbor model. Motivated by recent high-precision work on the square-lattice $J_1 - J_2$ next-nearest-neighbor model, which shows a direct transition from Néel order to a valence-bond solid without an intermediate spin liquid [1], we aimed to compute the ground-state staggered magnetization across these phase diagrams within Linear Spin-Wave Theory (LSWT). In the nearest-neighbor scenario, the magnetization was computed in the magnon ground state within the magnetic Brillouin zone [2], computing the integrals using Duffy-type coordinate transformations to regularize the infrared singularities at the Goldstone points [3]. This approach resembles accurately the known results for the unfrustrated 2D square [4] and 3D simple-cubic [5] antiferromagnets, obtaining magnetizations in excellent agreement with established values from more fancy methods as quantum Monte Carlo and series expansions broadly found in literature. Therefore, it is proposed that the established framework LSWT + Duffy-type transformations could be also extended to the frustrated next-nearest neighbor $J_1 - J_2$ scenarios [1, 6], mapping where long-range magnetic order survives or collapses as frustration is increased, and thereby providing a novel and simpler method to approach the stability of the magnetization in these canonical frustrated quantum magnets.

Keywords: Heisenberg antiferromagnet, frustrated magnetization, spin liquid, Linear Spin-Wave-Theory, Duffy transformation

Contents

1 Introduction

The stability of long-range antiferromagnetic order in quantum spin systems is a fundamental problem in condensed-matter physics, particularly in low-dimensional and weakly frustrated lattices, where understanding the nature of the ground state could have remarkable consequences for the high-temperature superconductivity. Spin-$\frac{1}{2}$ Heisenberg models on the two-dimensional square lattice and the three-dimensional simple-cubic lattice provide canonical cases for studying the interplay between quantum fluctuations and magnetic order [4,5]. Even in the unfrustrated nearest-neighbor case, zero-point quantum fluctuations strongly reduce the staggered magnetization from its classical value, a quantity that can be computed via the magnon dispersion within Linear Spin-Wave Theory (LSWT) [4], although leading to divergent integrals, the so-called infrared singularities at the Goldstone points, that makes the spin-wave expansion an asymptotic approach [7]. This *Individual Project in Physics* aimed to compute the ground-state staggered magnetization of square and cubic antiferromagnetic Heisenberg lattices within LSWT using Duffy-regularized integrals [3] in reciprocal space, finding values in agreement with established numerical benchmarks from quantum Monte Carlo and series expansion methods [4,5]. Building on this framework, we believe that this approach can be extended to the frustrated square-lattice next-nearest-neighbor J_1–J_2 Heisenberg model, motivated by recent high-precision studies showing a direct transition from Néel order to a valence-bond solid as frustration increases [1], making possible to analyze the stability of antiferromagnetic order and to identify the parameter regimes where long-range Néel order breaks down.

The present work has been organized as follows:

Section 2 introduces the nearest-neighbor Heisenberg model within LSWT, considering only the antiferromagnetic case where it has been showed the absence of magnetic ordering [8] (contrasting to the ferromagnetic case). The model is diagonalized by introducing the Holstein-Primakoff [9] and Bogoliubov transformations [10], finding the well-known magnon dispersion relation [11] for the 2D square and 3D simple-cubic lattices.

Section 3 covers briefly the definition of the Magnetic Brillouin zone (MBZ), a concept that emerges in the case of bipartite lattices, like in antiferromagnets. The dispersion relations for both cases (2D square and 3D simple-cubic lattices) is plotted within the MBZ.

In section 4 the staggered magnetization is computed analytically within LSWT approach, showing the origin of the divergences in the theory.

In section 5 relies the essence of this *Individual Project in Physics*. The Duffy transformations are applied for integration over the MBZ, showing explicitly how the computation of the staggered magnetization is effectively regularized.

Section 6 is for conclusions, and some numerical details on the Duffy-regularized integration is included in the Appendix A.

2 Model and Linear Spin–Wave dispersion

We consider the spin–S nearest–neighbor Heisenberg antiferromagnet on a bipartite lattice:

$$\hat{H} = J \sum_{\langle i,j \rangle} \hat{\boldsymbol{S}}_i \cdot \hat{\boldsymbol{S}}_j, \qquad J > 0 \tag{1}$$

where $\langle i, j \rangle$ denotes nearest neighbors and the lattice is either:

- square (2D) with lattice constants a, b and coordination number $q = 4$,
- simple cubic (3D) with lattice constants a, b, c and coordination number $q = 6$.

The classical ground state is a Néel configuration with antiparallel spins on sublattices A and B [11].

2.1 Holstein–Primakoff and Bogoliubov transformation

Within Linear Spin-Wave-Theory approach, one introduces Holstein–Primakoff bosons $\hat{a}_i$ ($i \in A$) and $\hat{b}_j$ ($j \in B$), expanding the spin operators to leading order in $1/S$. After Fourier transform, a quadratic order expansion, and a Bogoliubov rotation, the Hamiltonian becomes diagonal in terms of magnon operators $\hat{\alpha}_{\boldsymbol{k}}$:

$$\hat{H} = E_0 + \sum_{\boldsymbol{k}} \varepsilon_{\boldsymbol{k}}\, \hat{\alpha}^{\dagger}_{\boldsymbol{k}} \hat{\alpha}_{\boldsymbol{k}} \tag{2}$$

With a one–magnon dispersion of the form:

$$\varepsilon_{\boldsymbol{k}} = qJS\sqrt{1 - \gamma^2_{\boldsymbol{k}}} \tag{3}$$

The structure factor $\gamma_{\boldsymbol{k}}$ depends on the lattice geometry:

$$\gamma_{\boldsymbol{k}} := \frac{1}{q} \sum_{\boldsymbol{\delta}} e^{i\boldsymbol{k}\cdot\boldsymbol{\delta}} \tag{4}$$

2.2 2D square lattice

For the 2D square lattice, the primitive vectors are given by $\boldsymbol{a}_x = a\,\hat{\boldsymbol{x}}$, $\boldsymbol{a}_y = b\,\hat{\boldsymbol{y}}$, with nearest–neighbor vectors $\boldsymbol{\delta} \in \{\pm\boldsymbol{a}_x, \pm\boldsymbol{a}_y\}$ and coordination number $q = 4$.

Then, the structure factor can be written as:

$$\gamma^{(\mathrm{2D})}_{\boldsymbol{k}} = \frac{1}{q} \sum_{\boldsymbol{\delta}} e^{i\boldsymbol{k}\cdot\boldsymbol{\delta}} = \frac{1}{4}\Big(e^{ik_x a} + e^{-ik_x a} + e^{ik_y b} + e^{-ik_y b}\Big) = \frac{1}{2}\big(\cos k_x a + \cos k_y b\big) \tag{5}$$

Substituting into (3) yields to the 2D magnon dispersion relation:

$$\varepsilon^{(\mathrm{2D})}_{\boldsymbol{k}} = 4JS\sqrt{1 - \gamma^{(\mathrm{2D})\,2}_{\boldsymbol{k}}} = 4JS\sqrt{1 - \frac{1}{4}\big(\cos k_x a + \cos k_y b\big)^2} \tag{6}$$

And considering spin $S = \frac{1}{2}$:

$$\varepsilon^{(\mathrm{2D})}_{\boldsymbol{k}} = 2J\sqrt{1 - \frac{1}{4}\big(\cos k_x a + \cos k_y b\big)^2} \tag{7}$$

This form is gonna be used for the numerical computations.

2.3 3D simple-cubic lattice

For the 3D simple–cubic lattice, the primitive vectors are $\boldsymbol{a}_x = a\,\hat{\boldsymbol{x}},\ \boldsymbol{a}_y = b\,\hat{\boldsymbol{y}},\ \boldsymbol{a}_z = c\,\hat{\boldsymbol{z}},$, where the nearest neighbors will be $\boldsymbol{\delta} \in \{\pm\boldsymbol{a}_x, \pm\boldsymbol{a}_y, \pm\boldsymbol{a}_z\}$ and coordination number $q = 6$.

Thus, the structure factor can be written as:

$$\gamma_{\boldsymbol{k}}^{(3\mathrm{D})} = \frac{1}{6}\sum_{\boldsymbol{\delta}} e^{i\boldsymbol{k}\cdot\boldsymbol{\delta}} = \frac{1}{3}\big(\cos k_x a + \cos k_y b + \cos k_z c\big) \tag{8}$$

Where the magnon dispersion relation can be computed straightforward:

$$\varepsilon_{\boldsymbol{k}}^{(3\mathrm{D})} = 6JS\sqrt{1-\gamma_{\boldsymbol{k}}^{(3\mathrm{D})\,2}} = 6JS\sqrt{1-\frac{1}{9}\big(\cos k_x a + \cos k_y b + \cos k_z c\big)^2} \tag{9}$$

Again, considering spin $S = \frac{1}{2}$:

$$\varepsilon_{\boldsymbol{k}}^{(3\mathrm{D})} = 3J\sqrt{1-\frac{1}{9}\big(\cos k_x a + \cos k_y b + \cos k_z c\big)^2} \tag{10}$$

which is the form considering in the numerical computations.

3 Magnetic Brillouin zone

For a bipartite lattice with Néel order, the natural Brillouin zone for spin–wave excitations is the *magnetic Brillouin zone* (MBZ) [2], which is half of the original Brillouin zone. For hypercubic lattices it is convenient to describe the MBZ as an ℓ^1–ball in reciprocal space.

Defining the *edge radius* as:

$$k_x^{\max} = \frac{\pi}{a}, \qquad k_y^{\max} = \frac{\pi}{b}, \qquad k_z^{\max} = \frac{\pi}{c} \tag{11}$$

In general, $k_j^{\max} = \pi/a_j$ for each lattice direction.

3.1 2D case: diamond MBZ

In two dimensions the MBZ can be written as:

$$\mathcal{D}_2 = \left\{(k_x, k_y) \in \mathbb{R}^2 \ :\ \frac{|k_x|}{k_x^{\max}} + \frac{|k_y|}{k_y^{\max}} \le 1\right\} \tag{12}$$

which is a diamond (a rotated square) inscribed in the rectangle $[-k_x^{\max}, k_x^{\max}] \times [-k_y^{\max}, k_y^{\max}]$.

In Figure 1 are plotted the disperssion relation (energy eigenvalues given in (7)) in the MBZ. Notice the energy eigenvalues are scaled in terms of the spin-coupling energy J.

In Figure 2 the energy-scaled value is shown, for a path within the diamond MBZ, along the highest symmetry points: $\Gamma = (0,0)$, $X = (\frac{\pi}{a}, 0)$, and $M = (\frac{\pi}{2a}, \frac{\pi}{2b})$.

3.2 3D case: octahedron MBZ

In three dimensions the MBZ is an octahedron:

$$\mathcal{D}_3 = \left\{(k_x, k_y, k_z) \in \mathbb{R}^3 \ :\ \frac{|k_x|}{k_x^{\max}} + \frac{|k_y|}{k_y^{\max}} + \frac{|k_z|}{k_z^{\max}} \le 1\right\} \tag{13}$$

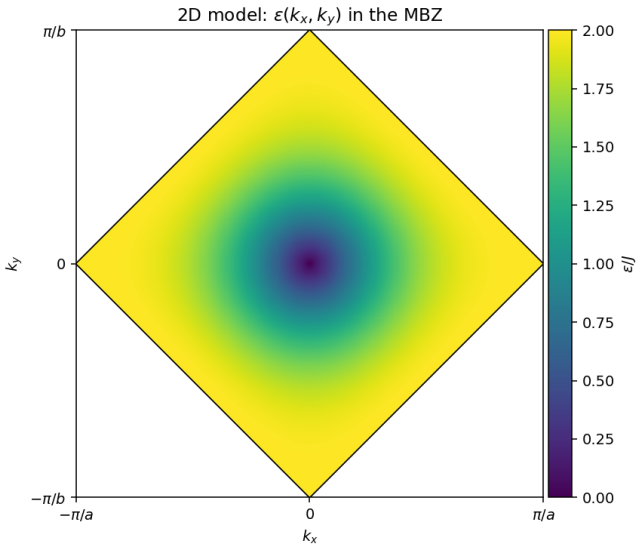

(a) Colour map of the energy eigenvalues in reciprocal space, for the square lattice Heisenberg antiferromagnet, in the MBZ.

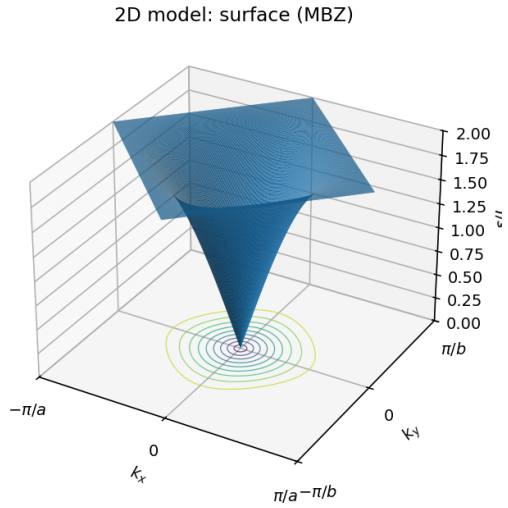

(b) Energy eigenvalues surface in reciprocal space, for the the square lattice Heisenberg antiferromagnet.

Figure 1: Disperssion relation in the MBZ for the 2D case.

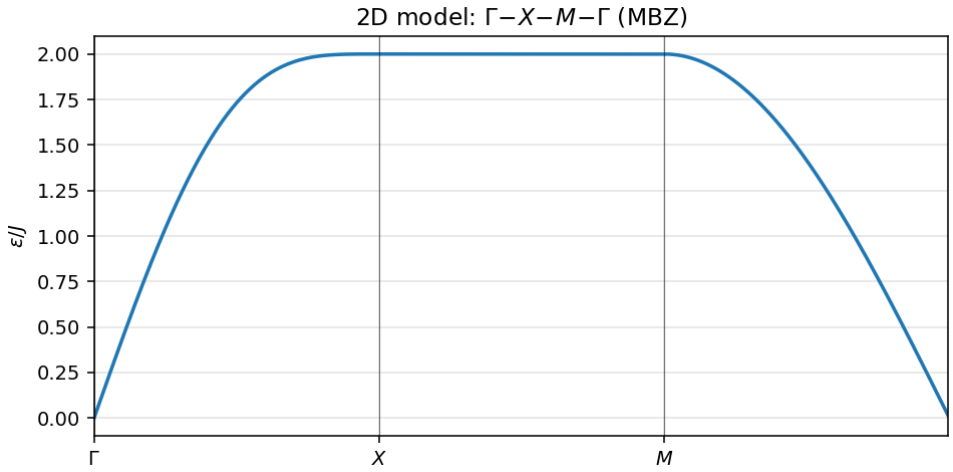

Figure 2: Path along the highest symmetry points inside the MBZ, for the square lattice Heisenberg antiferromagnet.

Where cross–sections at fixed k_z resemble the 2D diamonds, shrinking to a point as $|k_z| \to k_z^{\max}$.

In Figure 3 are plotted the disperssion relation (energy eigenvalues given in (10)) in the MBZ. Notice that $k_z = 0$ determines the center of the octahedron, which turns to be also a diamond as in the 2D case. Again the energy eigenvalues are scaled in terms of the spin-coupling energy J.

In Figure 4 the energy-scaled value is shown, for a path within the diamond MBZ, along the highest symmetry points: $\Gamma = (0,0,0)$, $X = (\frac{\pi}{a}, 0, 0)$, $M = (\frac{\pi}{2a}, \frac{\pi}{2b}, 0)$, and $R = (0, 0, \frac{\pi}{c})$ which corresponds to the edge of the octahedron.

A remark is that the MBZ can be decomposed into $2^d d!$ congruent simplices:

- In 2D: $2^2 \cdot 2! = 8$ congruent right triangles.

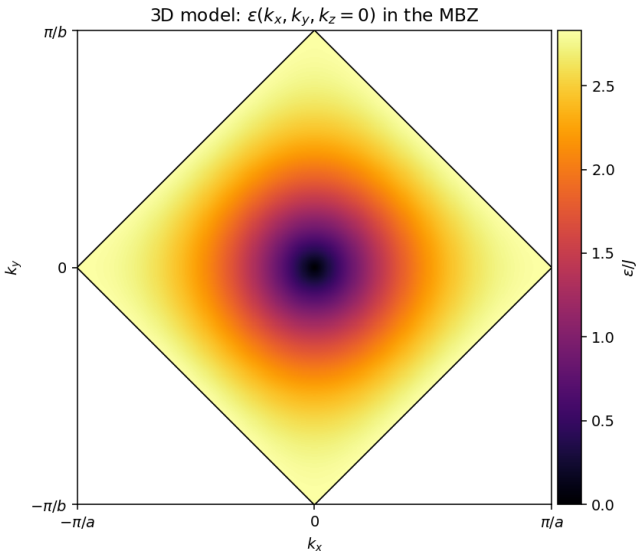

(a) Colour map of the energy eigenvalues in reciprocal space, for the cubic lattice Heisenberg antiferromagnet, in the MBZ.

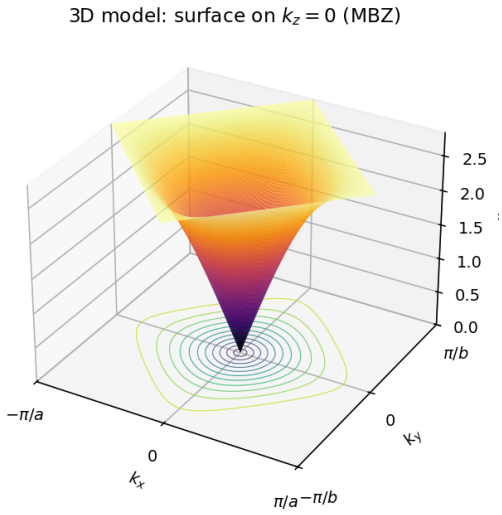

(b) Energy eigenvalues surface in reciprocal space, for the the cubic lattice Heisenberg antiferromagnet.

Figure 3: Disperssion relation in the MBZ for the 3D case.

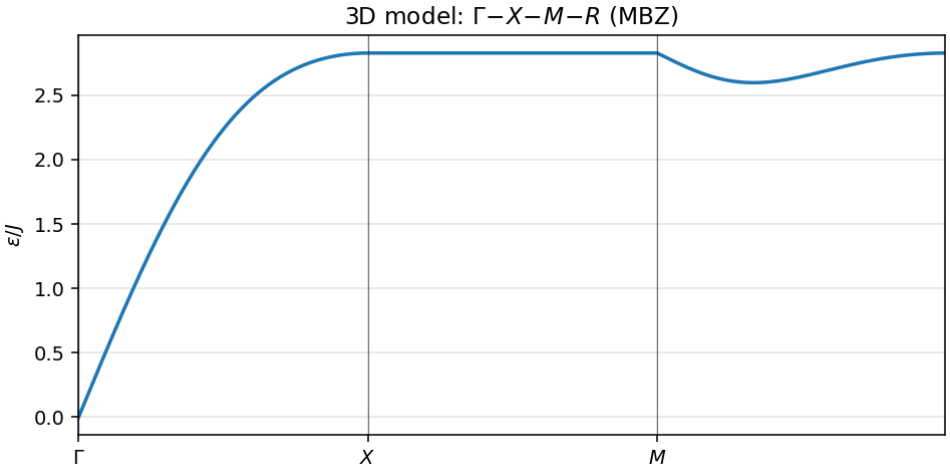

Figure 4: Path along the highest symmetry points inside the MBZ, for the square lattice Heisenberg antiferromagnet.

- In 3D: $2^3 \cdot 3! = 48$ congruent tetrahedra.

This decomposition is essential for the Duffy transformation, since is gonna be a factor that simplifies the integration domain.

4 Staggered Magnetization

Within Linear Spin-Wave-Theory, the expectation value of the z–component of the spin on a sublattice–A site can be computed as:

$$\begin{aligned}\langle \hat{S}_i^z \rangle &= \langle \Psi_G | \hat{S}_i^z | \Psi_G \rangle \\ &= \langle \Psi_G | S - \hat{a}_i^\dagger \hat{a}_i | \Psi_G \rangle\end{aligned} \tag{14}$$

Where $\hat{a}_i, \hat{a}_i^\dagger$ are the Holstein–Primakoff bosons on sublattice A, and $|\Psi_G\rangle$ is the ground state in the magnon Hamiltonian (2), such that:

$$\begin{aligned}\hat{\alpha}_{\boldsymbol{k}} |\Psi_G\rangle &= 0 \\ \hat{\beta}_{\boldsymbol{k}} |\Psi_G\rangle &= 0\end{aligned} \tag{15}$$

By Fourier-transforming, and introducing the Bogoliubov transformations, the staggered magnetization can be computed as:

$$\begin{aligned}\langle \hat{S}_i^z \rangle &= \langle \Psi_G | S - \hat{a}_i^\dagger \hat{a}_i | \Psi_G \rangle \\ &= S - \langle \Psi_G | \hat{a}_i^\dagger \hat{a}_i | \Psi_G \rangle \\ &= S - \langle \Psi_G | \frac{2}{N} \sum_{\boldsymbol{k},\boldsymbol{k'}} e^{-i(\boldsymbol{k}-\boldsymbol{k'})\cdot \boldsymbol{r}_i} \hat{a}_{\boldsymbol{k'}}^\dagger \hat{a}_{\boldsymbol{k}} | \Psi_G \rangle \\ &= S - \frac{2}{N} \langle \Psi_G | \sum_{\boldsymbol{k},\boldsymbol{k'}} e^{-i(\boldsymbol{k}-\boldsymbol{k'})\cdot \boldsymbol{r}_i} (u_{\boldsymbol{k'}}^* \hat{\alpha}_{\boldsymbol{k'}}^\dagger + v_{\boldsymbol{k'}}^* \hat{\beta}_{-\boldsymbol{k'}}) (u_{\boldsymbol{k}} \hat{\alpha}_{\boldsymbol{k}} + v_{\boldsymbol{k}} \hat{\beta}_{-\boldsymbol{k}}^\dagger) | \Psi_G \rangle \\ &= S - \frac{2}{N} \sum_{\boldsymbol{k},\boldsymbol{k'}} e^{-i(\boldsymbol{k}-\boldsymbol{k'})\cdot \boldsymbol{r}_i} v_{\boldsymbol{k'}}^* v_{\boldsymbol{k}} \delta_{-\boldsymbol{k'},-\boldsymbol{k}} \langle \Psi_G | \Psi_G \rangle \\ &= S - \frac{2}{N} \sum_{\boldsymbol{k}} |v_{\boldsymbol{k}}|^2\end{aligned} \tag{16}$$

Where the orthogonality relation for the bipartite lattice has been applied, and $v_{\boldsymbol{k}}$ is the Bogoliubov coefficient.

In momentum space and in the thermodynamic limit $T = 0$, this expectation value can be computed over the MBZ:

$$\frac{2}{N} \sum_{\boldsymbol{k} \in \mathrm{MBZ}} |v_{\boldsymbol{k}}|^2 \quad \longrightarrow \quad \frac{1}{(2\pi)^d} \int_{\mathrm{MBZ}} |v_{\boldsymbol{k}}|^2 \, d^d k, \tag{17}$$

For the Antiferromagnetic Heisenberg model:

$$|v_{\boldsymbol{k}}|^2 = \frac{1}{2} \left(\frac{1}{\sqrt{1 - \gamma_{\boldsymbol{k}}^2}} - 1 \right) \equiv f(\boldsymbol{k}) \tag{18}$$

Thus, in d dimensions,

$$\boxed{\langle \hat{S}_i^z \rangle = S - \frac{1}{(2\pi)^d} \int_{\mathrm{MBZ}} f(\boldsymbol{k}) \, d^d k,} \tag{19}$$

with

$$f(\boldsymbol{k}) = \frac{1}{2} \left(\frac{1}{\sqrt{1 - \gamma_{\boldsymbol{k}}^2}} - 1 \right), \qquad \gamma_{\boldsymbol{k}} = \begin{cases} \gamma_{\boldsymbol{k}}^{(2\mathrm{D})} & \text{square,} \\ \gamma_{\boldsymbol{k}}^{(3\mathrm{D})} & \text{simple cubic.} \end{cases} \tag{20}$$

Near the ordering vector $\boldsymbol{k} = 0$, $1 - \gamma_{\boldsymbol{k}}^2 \sim C|\boldsymbol{k}|^2$, therefore

$$f(\boldsymbol{k}) \sim \frac{\text{cte}}{|\boldsymbol{k}|}, \qquad (\boldsymbol{k} \to 0) \tag{21}$$

which is integrable in $d = 2, 3$, but leads to a *corner singularity*, the so-called infrared singularities at the Goldstone points, that must be handled carefully in numerical integration.

5 Duffy transforms for integration over the MBZ

Now, let's explain how to convert the integral over the d-dimensional MBZ:

$$I_d = \int_{\text{MBZ}} f(\boldsymbol{k})\, d^d k \tag{22}$$

into an integral over the unit hypercube $[0, 1]^d$ using *Duffy transformation* [3]. This yields an integrand which is regular at the origin, allowing high–order Gauss–Legendre quadrature and succesful numerical computation.

5.1 Symmetry reduction to one simplex

Recall that the MBZ is the ℓ^1–ball (diamond in 2D, octahedron in 3D) defined as:

$$\mathcal{D}_d = \left\{ \boldsymbol{k} : \sum_{j=1}^{d} \frac{|k_j|}{k_j^{\max}} \leq 1 \right\}, \qquad k_j^{\max} = \frac{\pi}{a_j} \tag{23}$$

Using symmetry under permutations and sign flips of components, the integration domain can be simplified to the *positive* simplex:

$$T_d = \left\{ k_j \geq 0,\ \sum_{j=1}^{d} \frac{k_j}{k_j^{\max}} \leq 1 \right\} \tag{24}$$

Since there are 2^d choices of signs and $d!$ permutations of the axes, then the integral can be written as:

$$\int_{\mathcal{D}_d} f(\boldsymbol{k})\, d^d k = 2^d d! \int_{T_d} f(\boldsymbol{k})\, d^d k \tag{25}$$

Explicitly:

$$\text{SF}_2 = 2^2 \cdot 2! = 8, \qquad \text{SF}_3 = 2^3 \cdot 3! = 48. \tag{26}$$

5.2 2D Duffy transform (triangle)

In the 2D square lattice, the MBZ is a diamond as it was discussed in Section 3. Therefore, the simplex is the triangle defined by:

$$\begin{aligned} T_2 &= \left\{ (k_x, k_y) : k_x, k_y \geq 0,\ \frac{k_x}{k_x^{\max}} + \frac{k_y}{k_y^{\max}} \leq 1 \right\} \\ &= \left\{ (k_x, k_y) : k_x, k_y \geq 0,\ \frac{k_x}{\pi/a} + \frac{k_y}{\pi/b} \leq 1 \right\} \end{aligned} \tag{27}$$

Let's introduce the parameters $(r, s) \in [0, 1]^2$, and define:

$$\boxed{k_x = k_x^{\max} r, \qquad k_y = k_y^{\max} r\, s} \tag{28}$$

Then, it is straightforward to check that this parameterization indeed resemble the positive triangle defined by $k_x, k_y \geq 0$:

$$\frac{k_x}{k_x^{\max}} + \frac{k_y}{k_y^{\max}} = r + rs = r(1 + s) \geq 0$$

Now, the Jacobian matrix associated to this transformation can be computed as:

$$\begin{aligned} J = \begin{pmatrix} \partial k_x/\partial r & \partial k_x/\partial s \\ \partial k_y/\partial r & \partial k_y/\partial s \end{pmatrix} &= \begin{pmatrix} k_x^{\max} & 0 \\ -k_y^{\max} s & k_y^{\max}(1 - r) \end{pmatrix} \\ &= \begin{pmatrix} \pi/a & 0 \\ \pi/b\ \ s & \pi/b\ \ r \end{pmatrix}, \end{aligned} \tag{29}$$

Thus the jacobian is given by:

$$\boxed{|\det J| = \frac{\pi^2}{ab} r} \tag{30}$$

Therefore, when evaluating the integral in (19), for two dimensions, and in the new parameterization:

$$\int_{T_2} f(k_x, k_y)\, dk_x\, dk_y = \int_0^1 \int_0^1 f\left(k_x^{\max} r,\ k_y^{\max} rs\right) |\det J|\, ds\, dr \tag{31}$$

Restoring the symmetry factor given in (25), and invoking the approximation in (21), it can be argued that the divergence is regularized by the Duffy transformation:

$$\begin{aligned} I_2 &= \int_{\mathcal{D}_2} f(\boldsymbol{k})\, d^2k \\ &= 8 \int_0^1 \int_0^1 f\left(k_x^{\max} r,\ k_y^{\max} rs\right) |\det J|\, ds\, dr \\ &\approx 8 \int_0^1 \int_0^1 \frac{1}{\sqrt{k_x^2 + k_y^2}} \frac{\pi^2}{ab} r\, ds\, dr \\ &\approx 8 \int_0^1 \int_0^1 \frac{1}{\frac{\pi}{ab} r \sqrt{b^2 + a^2 s^2}} \frac{\pi^2}{ab} r\, ds\, dr \\ &\approx 8 \int_0^1 \int_0^1 \frac{\pi}{\sqrt{b^2 + a^2 s^2}}\, ds\, dr \end{aligned} \tag{32}$$

This integral is well defined and does not diverge. However, because of the approximation of the integrand this does not lead to the actual corrections of the staggered magnetization, where the full function in (20) must be integrated. This can be done numerically (see Section A), which lead to the result:

$$\langle \hat{S}_i^z \rangle_{2\mathrm{D}} = S - \frac{I_2}{(2\pi)^2} \approx 0.30341144 \tag{33}$$

Where the spin has been considered to be $S = 1/2$. These results are in well agreement with the ones found in [2].

5.3 3D Duffy transform (tetrahedron)

For the 3D simple-cubic lattice, the MBZ was found to be a octahedron, then the simplex is defined as a tetrahedron:

$$T_3 = \left\{ (k_x, k_y, k_z) : k_x, k_y, k_z \geq 0,\ \frac{k_x}{k_x^{\max}} + \frac{k_y}{k_y^{\max}} + \frac{k_z}{k_z^{\max}} \leq 1 \right\} \tag{34}$$

We now map $(r, s, t) \in [0, 1]^3$ to (k_x, k_y, k_z) as

$$\boxed{\begin{aligned} k_x &= k_x^{\max}\, r, \\ k_y &= k_y^{\max}\, r\, s, \\ k_z &= k_z^{\max}\, r s\, t. \end{aligned}} \tag{35}$$

Again $k_x, k_y, k_z \geq 0$ and

$$\frac{k_x}{k_x^{\max}} + \frac{k_y}{k_y^{\max}} + \frac{k_z}{k_z^{\max}} = r + rs + rst = r(1 + s(1 + t)) \geq 0 \tag{36}$$

The Jacobian is now 3×3, whose determinant can be computed explicitly, finding the jacobian:

$$\boxed{|\det J| = k_x^{\max} k_y^{\max} k_z^{\max}\, r^2 s} \tag{37}$$

Hence, the integral over the simplex can be written as:

$$\int_{T_3} f(\boldsymbol{k})\, d^3k = \int_0^1 \int_0^1 \int_0^1 f\big(k_x^{\max} r,\ k_y^{\max} rs,\ k_z^{\max} rst\big)\, k_x^{\max} k_y^{\max} k_z^{\max}\, r^2 s\, dt\, ds\, dr \tag{38}$$

And by considering the symmetry factor, it is found the integral over the MBZ:

$$\boxed{I_3 = \int_{\mathcal{D}_3} f(\boldsymbol{k})\, d^3k = 48 \int_0^1 \int_0^1 \int_0^1 f\big(k_x^{\max} r,\ k_y^{\max} rs,\ k_z^{\max} rst\big)\, k_x^{\max} k_y^{\max} k_z^{\max}\, r^2 s\, dt\, ds\, dr} \tag{39}$$

So, when considering spin $S = 1/2$, it was computed the staggered magnetization to be:

$$\langle \hat{S}_i^z \rangle_{3\mathrm{D}} = S - \frac{I_3}{(2\pi)^3} \approx 0.42164229 \tag{40}$$

Which is in excellent agreement with the values reported in literature [5].

6 Conclusions

Staggered magnetization was computed for the 2D square ($\langle S \rangle_{2D} \approx 0.30341144$) and 3D simple-cubic ($\langle S \rangle_{3D} \approx 0.42164229$) Heisenberg antiferromagnetic models, within Linear Spin-Wave-Theory (LSWT), finding excellent agreement with the values reported broadly in literature that employ other methods as series expansions and Monte Carlo simulations. This was successfully done by exploiting the power of Duffy transformations, used in order to regularize the integrals resulting from the staggered magnetization in the Heisenberg antiferromagnets.

In addition, the LSWT approach to the Heisenberg antiferromagnetic models was fully presented for both cases, showing the magnon dispersion relations, and finding that the Magnetic Brillouin Zone for the 2D square lattice resembles a diamond, whereas for the 3D simple-subic is an octahedron whose cross sections are diamonds as in the 2D case.

Finally, we argue that this framework LSWT + Duffy regularization could be also extended to the frustrated scenarios in the next-nearest-neighbor $J_1 - J_2$ models, identifying the phase transitions in which long-range magnetic order survives or collapses as frustration increases, thus providing a new simple method to approach the stability of the magnetization in these canonical frustrated scenarios.

References

[1] X. Qian and M. Qin. Direct transition from néel order to valence-bond solid in the square-lattice j_1–j_2 heisenberg model. *Physical Review B*, 109:L161103, 2024.

[2] Guillermo E Castilla and Sudip Chakravarty. Spin-wave expansion of the staggered magnetization of a square-lattice heisenberg antiferromagnet at t= 0. *Physical Review B*, 43(16):13687, 1991.

[3] SE Mousavi and N Sukumar. Generalized duffy transformation for integrating vertex singularities. *Computational Mechanics*, 45(2):127–140, 2010.

[4] D. A. Huse. Ground-state staggered magnetization of two-dimensional antiferromagnets. *Physical Review B*, 37:2380–2382, 1988.

[5] J. Oitmaa, C. J. Hamer, and W. Zheng. Series expansions for quantum antiferromagnets on the simple-cubic lattice. *Physical Review B*, 50:3877–3887, 1994.

[6] P Chandra and B Doucot. Possible spin-liquid state at large s for the frustrated square heisenberg lattice. *Physical Review B*, 38(13):9335, 1988.

[7] Freeman J Dyson. General theory of spin-wave interactions. *Physical review*, 102(5):1217, 1956.

[8] Michael Karbach, Kun Hu, and Gerhard Muller. Introduction to the bethe ansatz ii. *arXiv preprint cond-mat/9809163*, 1998.

[9] Theodore Holstein and Henry Primakoff. Field dependence of the intrinsic domain magnetization of a ferromagnet. *Physical Review*, 58(12):1098, 1940.

[10] Nikolai Bogoliubov. On the theory of superfluidity. *J. Phys*, 11(1):23, 1947.

[11] Ryogo Kubo. The spin-wave theory as a variational method and its application to antiferromagnetism. *Reviews of Modern Physics*, 25(1):344, 1953.

A Appendix: Numerical integration over the Magnetic Brillouin Zone

Now, let's describe the numerical quadrature based on the Duffy mappings (31) and (39).

A.1 Gauss–Legendre implementation on the unit segment $[0, 1]$

Let $(x_i, w_i)_{i=1}^n$ be the Gauss–Legendre nodes and weights on $[-1, 1]$. To obtain a quadrature on $[0, 1]$, the following map is defined:

$$t_i = \frac{x_i + 1}{2}, \qquad \tilde{w}_i = \frac{w_i}{2}. \tag{41}$$

In Python code:

```
x, w = np.polynomial.legendre.leggauss(n)
t = 0.5*(x + 1.0)
wt = 0.5*w
```

A.2 2D quadrature on the MBZ (diamond)

Combining the Duffy transform and tensor Gauss–Legendre, the 2D MBZ integral is approximated by:

$$I_2 \approx 8 \sum_{i=1}^{n} \sum_{j=1}^{n} f\big(k_x^{\max} r_i,\ k_y^{\max} r_i s_j\big)\, k_x^{\max} k_y^{\max} r_i\, \tilde{w}_i \tilde{w}_j. \tag{42}$$

In vectorized Python notation:

```
r, wr = gauss_legendre_on_01(n)
s, ws = gauss_legendre_on_01(n)
R, S  = np.meshgrid(r, s, indexing='ij')
WR,WS = np.meshgrid(wr, ws, indexing='ij')

kx  = kxmax * R
ky  = kymax * R * S
jac = kxmax * kymax *  R

val = f(kx, ky) * jac
I2  = 8.0 * np.sum(val * WR * WS)
```

Where $f(k_x, k_y)$ is given by (18) with $\gamma_{\boldsymbol{k}}^{(2D)}$.

A.3 3D quadrature on the MBZ (octahedron)

Similarly, using the mapping (35), the 3D MBZ integral can be approximated as:

$$I_3 \approx 48 \sum_{i,j,k=1}^{n} f\Big(k_x^{\max} r_i,\, k_y^{\max}(1-r_i)s_j,\, k_z^{\max}(1-r_i)(1-s_j)t_k\Big) k_x^{\max} k_y^{\max} k_z^{\max} (1-r_i)^2 (1-s_j)\, \tilde{w}_i \tilde{w}_j \tilde{w}_k. \tag{43}$$

In Python code:

```
r, wr = gauss_legendre_on_01(n)
s, ws = gauss_legendre_on_01(n)
t, wt = gauss_legendre_on_01(n)

R,S,T  = np.meshgrid(r, s, t, indexing='ij')
WR,WS,WT = np.meshgrid(wr, ws, wt, indexing='ij')

kx  = kxmax * R
ky  = kymax * (1.0 - R) * S
kz  = kzmax * (1.0 - R) * (1.0 - S) * T
jac = (kxmax * kymax * kzmax) * (1.0 - R)**2 * (1.0 - S)

val = f(kx, ky, kz) * jac
I3  = 48.0 * np.sum(val * WR * WS * WT)
```

where $f(k_x, k_y, k_z)$ uses $\gamma_{\boldsymbol{k}}^{(3D)}$.